# A Model for the Direct Gain Passive Solar Room Facilitating Performance Analysis of Fenestration Strategies

**G. Newsham** **N. Baker, Ph.D.**

ABSTRACT

The direct gain space is probably the simplest and cheapest way of exploiting the heat of the sun in a domestic building. The most suitable choice of space, especially in low-cost buildings, is the living room, perhaps the only space of any size capable of being placed on the south facade. Occupant comfort should be the prime consideration in the design of a direct gain living room and a desire to lower the energy bill should not jeopardize comfort criteria. In an attempt to assess the interaction of comfort and energy cost, a detailed, mainframe-based thermal model is being developed. Temperatures are calculated every 15 minutes at 144 nodes within a single room. Glazing area and geometry can be varied; glazing strategies are compared on the basis of both auxiliary heat consumed and a comfort score.

## INTRODUCTION

There is certainly no shortage of mathematical models that attempt to simulate the heat transfer and thermal conditions within buildings (CEC 1986; Littler 1982; Clarke 1985); however, this does not mean that the task of capable thermal modeling has been solved. Intermodel comparative studies (Judkoff 1988) indicate differences of up to 20% in annual auxiliary heating requirements and 14°F (8°C) in temperature in the direct gain zone; these disparities become greater as more sun is allowed into the building - a significant source of worry when such programs are intended for passive solar calculations! It is common for only a single air node to be considered and, with a few exceptions (Alder et al. 1984; Heerwagen et al. 1979), little regard is given to occupant comfort. If an attempt to quantify comfort is made at all, the result is not used as a major indicator of a building's performance.

The model presented here seeks to accurately represent thermal comfort, both temporally and spatially, and make this the prime influence in the evaluation of design performance. To do this it is necessary to produce a nodal network capable of resolving spatially significant effects and to ensure that the inputs to the model are, if necessary, spatially variant. For example, sunpatch tracking is employed and the building's microclimate may be represented.

In evaluating human comfort, the local air temperature has approximately the same importance as the mean radiant temperature (MRT) and thus it is imperative that some attempt be made to model the spatial variations in room air temperature. Stratification is a familiar concept (Howarth 1985; Liebecq and Marret 1984), that is rarely modeled, and horizontal air temperature gradients may also be significant (Ruberg 1979).

## MODEL DESCRIPTION

*FENESTRA*, the thermal model that has been developed, is a 144-node resistance network with timesteps of 15 minutes. One hundred seventeen nodes refer to the building materials that form the boundary of the room (walls, floor, ceiling), and the room air (with some allowance for furnishings, etc.) is divided into another 27 equal volume nodes. Floor and ceiling - like non-south walls - have a two-node (surface+buried) thickness, the south external wall has a three-node (external surface+buried+internal surface) thickness. Any of the south wall nodes may be glazing.

Guy Newsham, Graduate Student, Martin Centre for Architectural and Urban Studies, University of Cambridge; Nick Baker, Director, Martin Centre for Architectural and Urban Studies, University of Cambridge.

## Model Limitations

It is obvious that the model has several limitations. First, only south-facing rooms are considered, with the south-facing wall being the only exterior wall (hence its three-node thickness). This is not a very serious restriction since, especially in the U.K., orientations away from south, on conventional sites, offer few advantages. In some cases of built low-cost housing either east or west walls are exterior walls, though they are seldom glazed. Second, the glazing on the south wall is not continuously variable but must follow nodal lines (0% to 100% of the south wall in 11.1% increments). Third, there is no explicit interaction between this room and the rest of the building of which it is a part. That is, there is no net heat gain from the rooms surrounding the modeled room. This is not too poor an approximation in thermostated buildings. Fourth, only rectangular room geometries are considered. While few living rooms may be perfectly rectangular, few will be far from it and this simplification greatly facilitates radiative exchanges and sunpatch tracking.

## Inputs and Outputs

On running the model, the user is asked to input the name of pre-prepared files detailing the following: site latitude and longitude, room dimensions, room construction details, properties of the room contents, overhang design, local relief profile and wind sheltering, window permeability, thermostat setting and occupancy schedule, curtains/blinds/shades type and utilization schedule, and weather sequence.

Many options for each of the 10 choices may be prepared and thus a large variety of room types may be examined. A description of the files used during this particular problem is given later.

The outputs available from the model are also many and varied. The auxiliary energy supplied to maintain comfort is designed as the basic indicator of the design's performance but also available in graphical form are the temperatures of all nodes with time, a "human index" temperature at each air node, weather data, air change rates, an occupancy profile, predicted percentage of the population dissatisfied with the calculated thermal conditions at that time step (PPD), and wind and stack pressures.

## Heat Transfer Routines

Every attempt has been made to perform all model calculations from physical principles. If certain coefficients vary with time, temperature, or occupancy then every effort is made to quantify this variation. "Average factors" or "yearly coefficients" are avoided if at all possible. A brief description of the routines employed follows:

Heat transfer by conduction:

$$\Delta Q_{ba} = A_a h_{cond_{ba}} \Delta T_{ba} \Delta t \qquad (1)$$

where

$Q_{ba}$ = heat transferred from body b to body a (Btu)
$A_a$ = contact area ($ft^2$)
$h_{cond}$ = coefficient of conductive heat transfer ($Btu/ft^2 \cdot s \cdot {}^oF$)
$\Delta T_{ba}$ = temperature difference between the bodies in contact ($^oF$)
$\Delta t$ = timestep (s)

All transfers from surface to buried nodes are by conduction. Conductive transfer from floor to ground is also considered.

Heat transfer by radiation:

$$\Delta Q_{ba} = \sigma A_b F_{ba} \Delta t \left[ T_b^4 - T_a^4 \right] S \qquad (2)$$

where

$\Delta Q_{ba}$ = heat transferred from surface b to surface a (Btu)

$\sigma$ = Stefan-Boltzman constant =$5.67 \times 10^{-8}$ (Btu/ft$^2$·s·R$^4$)

$A_b$ = area of surface b (ft$^2$)

$F_{ba}$ = view factor - fraction of radiation emitted by surface b that is absorbed by surface a

T = surface temperature (R)

$\Delta t$ = timestep (s)

$S$ = obstruction fraction from shading and room contents

Exchanges are calculated between all 54 surface nodes, room contents, sky (Geiger 1965) and, if present, the overhang. A 54 by 54 view factor matrix is employed for the interior surface exchanges containing values that are exact and derived from the application of well-known formulae (Welty 1978).

Heat transfer by convection:

$$\Delta Q_{sa} = A_s h_{conv} b \Delta T_{sa} \Delta t \quad (3)$$

where

$\Delta Q_{sa}$ = heat transferred to air from a solid surface (Btu)

$A_s$ = area of convecting surface (ft$^2$)

$h_{conv}$ = coefficient of convective heat transfer (Btu/ft$^2$·s·$^o$F)

b = obstruction fraction via shading devices

$\Delta T_{sa}$ = surface to air temperature difference ($^o$F)

$\Delta t$ = timestep (s)

Many models ignore the fact that $h_{conv}$ is a function of temperature. However, *FENESTRA* employs the findings of Alamdari and Hammond (1983) supported by Martin and Watson (1988):

$$h_{conv} = \left[ \left(1.5(\Delta T/ht)^{0.25}\right)^6 + \left(1.23(\Delta T)^{0.33}\right)^6 \right]^{\frac{1}{6}} \quad (4)$$

for vertical surfaces of height ht and

$$h_{conv} = \left[ \left(1.4(\Delta T/L)^{0.25}\right)^6 + \left(1.63(\Delta T)^{0.33}\right)^6 \right]^{\frac{1}{6}} \quad (5)$$

for horizontal surfaces above or below non-stably stratified air (e.g., floor sunpatch below a cooler air layer) and

$$h_{conv} = 0.6\,(\Delta T/L)^{0.2} \quad (6)$$

for horizontal surfaces above or below stably stratified air (e.g., a warm ceiling above a cooler air layer)

where

L = 4 x surface area / surface perimeter (ft)

These calculations are performed at all interior surfaces in contact with room air and at external surfaces in contact with ambient air (in which case the convective transfer is boosted due to the effects of wind).

Infiltration is calculated in three parts (CEC 1986; ASHRAE 1977):

1. Through cracks in the window frames, which is dependent on wind pressure (in turn dependent on local terrain and the square of the wind speed), stack pressure (in turn dependent on building height), and the temperature difference between the room and ambient and window unit type.
2. Through the external walls, dependent on wind pressure and wall construction
3. Through open windows, which depends on the wind speed and direction and on the area of the window opening (in turn dependent on minimum air change rate requirement and room comfort

## Sunpatch Tracking

It is not sufficient to know merely the magnitude of the solar gain to the room; it would be beneficial to know on which surfaces the sun falls so that these surfaces may be designed to exploit the solar gains most efficiently and so that thermal comfort can be calculated spatially within the room.

Sunpatch tracking is facilitated by dividing each glazed node into 100 equal area segments. Solar position is calculated every timestep and a ray is considered to pass through the center of each segment. The interior wall node on which each ray falls is considered to gain 1% of the solar incident upon the south wall glazed node of the ray's origin once overhang and microclimate shadowing and the transmittance of the glazing (ASHRAE 1977) (not forgetting multiple internal reflections if double or triple glazing is utilized) are taken into account. Any reflectance from internal surfaces is considered non-directional and is distributed among internal nodes according to view factors.

## Daylighting

*FENESTRA* is able to predict daylight levels on a horizontal surface at the centre of any air node. The daylight factor is calculated following Hopkinson et al. (1966) and the contribution to the internal light level made by any direct beam radiation is approximated by treating the sunpatch as a light source located at floor level that reaches the horizontal surface by internal reflection. If the total daylight level is considered insuffiecient artificial lighting is activated and the casual gains from these fittings are added to the room's heat balance.

## Distribution of Air Temperatures

The distribution of air temperatures around the room is also important both in considering localized thermal comfort and convective heat transfer.

The method used in *FENESTRA* is very simple and yet is still able to reproduce the findings of Liebecq and Marret (1984), Ruberg (1979) and Martin (1988) both in the magnitude of the temperature gradients and in the effect on the gradient of radiator/sunpatch positions and ventilation rates. The three-layer vertical node distribution was chosen so that the typical "S" shape stratification curve (Figure 1) could be predicted (though in the model's case the zones are of equal height).

At a first level of approximation it is reasonable to assume that all positive heat inputs to the room air (via convection and ventilation) are considered to go to the upper air levels and all negative inputs (heat losses) to the lower air levels. However, the distribution of inputs must be considered since positive inputs entering at low levels (i.e., at a sunpatch) will give some positive heat input to lower air levels and oppose negative inputs from surfaces above. Then

$$\Delta T_{strat} = \frac{Q_{top} - Q_{bottom}}{\alpha} \qquad (7)$$

where

$\Delta T_{strat}$ = temperature increment over the mean air temperature due to stratification (F)
$Q_{top}$ = total heat inputs to the top of the room (Btu)
$Q_{bottom}$ = total heat inputs to the bottom of the room (Btu)
$\alpha$ = distribution constant (Btu/°F)

| | | |
|---|---|---|
| Tair-upper | = To + ΔTstrat | (8) |
| Tair-lower | = To - ΔTstrat | (9) |
| Tair-mid | = To | (10) |

$T_o$ is the average room air temperature and $\alpha$ is derived empirically to fit the data. The stratification profile is as shown in Figure 2.

Similarly, heat inputs are divided up at back and front of the room and east and west sides to produce horizontal air temperature gradients with a distribution constant again empirically derived. Note that no attempt is made to link the air nodes conductively.

## Comfort

Domestic buildings are not designed to be absolutely regulated boxes that consume the minimum amount of energy that is economically viable in maintaining a particular air temperature; they are intended to be occupied by humans and should be designed to perform most efficiently with respect to the wishes of these occupants. However, all too often modelers treat potential occupants as no more than metabolic heat generators, a handy means of offsetting heating season auxiliary energy demand.

Occupants will adjust the variables at their control, thermostat, lighting, ventilation, shading, clothing, etc. to ensure that they are comfortable and, since these adjustments have a bearing on the room's thermal performance, it is essential that any assessment of building performance include a comfort term.

The human body loses heat both radiatively and convectively by a number of different processes and therefore if we seek to represent the human thermal sensation by a single temperature it must accurately reflect the importance of these processes in a weighted mean of the temperatures that govern the rate of each heat loss. Humphreys (1974) suggests

$$T_{human} = 0.54T_{air} + 0.46T_{mrt} \quad (11)$$

where

$T_{air}$ = air temperature (°F)
$T_{mrt}$ = mean radiant temperature (°F)
$T_{human}$ = temperature "felt" by the human subject (°F)

Next, it is necessary to calculate at what value of $T_{human}$ the subjects will be most comfortable. After extensive trials in climate chambers Fanger produced a "heat balance on the body equation" adaptable to predict a $T_{human}$ which would, among a large population, produce the maximum number of "comfortable" subjects. These equations include terms for air temperature, MRT, humidity, air speed, and subject's clothing and metabolic rate. While based on a very detailed study of physiological response, Fanger's equation in its fullest form has several drawbacks. First, the subjects were predominantly college students in a non-domestic environment. Second, clothing and metabolic rate are extremely difficult to define adequately on a timestep basis. Third, if a thermostat is ever to be replaced by a "human comfort sensor", especially one with spatial sensitivity, the humidity and air speed must be measured spatially, not a very practical proposition in a domestic setting. Finally, it is assumed that the preferred state in which to be is one in which the total net heat to the body is zero which is not necessarily the case (Nevrala and Pimbert 1981).

Therefore a simplified equation for preferred temperature should be sought. Humphreys (1978) reports that 78% of the variation of preferred temperature can be accounted for by the change in the monthly mean outdoor temperature alone using

$$T_{pref} = 24.2 + 0.43(\theta_{amb} - 22)e^{-[(\theta_{amb}-22)/20\sqrt{2}]^2} \quad (12)$$

where

$T_{pref}$ = preferred temperature (°F)
$\theta_{amb}$ = monthly mean outdoor temperature (°F)

This may seem surprising bearing in mind the complexity implied by Fanger, however, metabolic rate and clothing are, in practice, inter-related, as are clothing and ambient temperature. Within buildings air velocity is often insignificant and the simplification may be even more valid in England where humidity is rarely a problem.

Carroll (1980) adopts a similar approach producing the even simpler

$$T_{pref} = PT_{base} + k(T_{human} - PT_{base}) - N \quad (13)$$

where

$PT_{base}$ = preferred temperature in mild weather (°F)
$T_{human}$ = human index temperature indoors (°F)
N = reduction in $T_{pref}$ for bedtime hours (°F)

Using Carroll's guidelines and UK preferences, we arrive at:

$$T_{pref} = 20.5 + 0.1T_{human} - N \quad (14)$$

where

N = 3.6 °F during bedtime hours

This equation is preferred because $T_{human}$ is used rather than a monthly mean of outdoor temperature, which is more appropriate to 15 minute timestep modeling and because Carroll's $T_{pref}$ refers explicitly to a $T_{human}$-type weighting of $T_{air}$ and $T_{mrt}$ whereas Humphreys' does not.

To relate $|T_{pref} - T_{human}|$ to the proportion of people dissatisfied with $T_{human}$, bearing in mind that $T_{pref}$ is only for the average of the population, Fanger's predicted percentage dissatisfied (PPD) curve in an approximate quadratic form is used, which is only noticeably different from Fanger's experimentally derived curves at temperatures very removed from $T_{pref}$ (Figure 3).

Following Carroll, an additional term can be added to the PPD predicted by the model for discomfort caused by variations in temperature. It has been demonstrated (McIntyre 1980) that temperature fluctuations introduce an uncomfortable thermal sensation and Carroll suggests a further "bother" effect due to the need to adjust clothing; adjusting thermostats, ventilation, and sunshading may also be "bothersome". The weighting of this term is dependent on timestep and is, at present, arbitrary. The weighting chosen for this study is effectively twice that chosen by Carroll; fluctuations in temperature over periods of 16 minutes (~1 timestep) are found to be particularly uncomfortable (McIntyre 1980).

$$PPD = 2(T_{human} - T_{pref})^2 + 5(\Delta T)^2 + 5 \quad (15)$$

where

$\Delta T$ = change in $T_{human}$ between timesteps (°F)

A flow diagram for *FENESTRA* is shown in Figure 4.

## ANALYSIS OF FENESTRATION STRATEGIES

The model *FENESTRA* allows the choice of many variables but, in this study, we seek only to analyze the effects of changing fenestration and so many of the input files are held constant. A description of the constants for this study is given below:

Site - Southeast England

Properties of the Room - The south facade of the room is 19.7 ft (6.0 m) long and 7.9 ft (2.4 m) high; the room is 13.1 ft (4.0 m) deep. The room furnishings, considered thermally coupled to the room air, are dark (solar absorptance = 0.7) with a thermal capacity five times that of the room air.

Room Construction - The construction of the room boundaries is typical for the kind of energy-efficient, but not "superinsulated" house in which passive solar may be utilized. Floor, ceiling, and north wall (internal) are solid, providing considerable thermal mass (Table 1). Window frames are normal leakage and are assumed to provide 10% obstruction to insolation entering the room. Glass used in all cases is clear, 0.25 in (6.25 mm) thick with a transmittance-to-perpendicular radiation of 85%. Window opening remains variable, being adjusted automatically in an attempt to maintain 0.5 air changes per hour and to reduce overheating.

Microclimate - The house is placed in a suburban setting with moderate shielding from winds but with no local relief high enough to provide solar shading at any time of the year.

Overhang - No overhang is employed.

Shades - If the global insolation falling on the south facade is greater than 95 Btu./ft$^2$.h (300 W/m$^2$) a sunshade of 48% opacity is employed.

Light Levels - Incandescent filament light sources of 60 W each are switched on when necessary to maintain a light level in the room of 28 lumen/ft$^2$ (300 lux).

Auxiliary Energy Input - To enable the comparison of glazing strategies in a simple way via auxiliary energy requirements but without compromising comfort considerations, the thermostat set temperature is taken to be $T_{pref} \pm 2.7$°F (9.5% PPD) for that particular timestep. Heating is only available during the hours of occupancy, which are chosen to be that of a working family - both parents working office hours and children, if any, at school; 6:00 to 8:30 a.m. and 4:30-11:00 p.m. (between 11:00 p.m. and 6:00 a.m. the heating is assumed to be off in preparation for and during sleep). The method of heat input is via a heated panel at the bottom southwest corner of the west wall.

Casual gains, up to a maximum of 860 Btu/h (250 W) are included in a simple, occupancy-dependent profile assuming that the room is independent of zones of high casual gains such as the kitchen.

Weather Data - Three days per month were chosen from the climate file for Kew, 1969 - an average temperature day, an above-average temperature day and a below average temperature day. The days were selected so that their average temperatures, insolation, and wind velocity were close to the average for the month. Table 2 compares the 36-day sample with the whole year-data.

Wind speed is extremely difficult to sample correctly since it fluctuates in both magnitude and direction; we are only interested in the wind component perpendicular to the south facade and therefore didn't worry unduly about inaccuracies in this regard. It is hoped that the inevitable discontinuities between the sample days do not affect the results too much; fortunately, these discontinuities occur at midnight when the impact is minimized.

The variations in window strategies are single, double, or triple glazing; glazed area of the south facade; and the geometric arrangement of the glazed elements on the south facade.

The outputs from the model on which the assessment of the glazing strategies is made are threefold: (i) auxiliary energy consumed in an attempt to maintain the comfort temperature and light level during the occupancy period, (ii) % time during which the 10% PPD limit is exceeded due to overheating ($PPD_{10}^+$), and (iii) % time during which the 10% PPD limit is exceeded due to underheating ($PPD_{10}^-$).

In cases (ii) and (iii) a weighting factor of 0.33 is applied to periods when the thermostat is off. The weighting factor should not be 0 since occupants occasionally may be present during these periods and during weekends and because temperature protection may be required for plants or damp protection sought for timber furniture and fittings.

The viewpoint for all runs was considered to be at the centre of the room. For annual runs no allowance for direct radiation onto occupants is made, a reasonable simplification considering the occupancy profile adopted.

## RESULTS

### Single, Double, and Triple Glazing

The first series of runs was designed to evaluate the significance on the room's performance of the number of layers of glass at a glazed node. Glazed area (22% of the south facade) and placement (upper central) were kept constant and the model was run for single, double (0.4 in air gap), and triple (2 by 0.2 in air gaps) glazing; the results are shown in Figure 5.

As might be expected, double glazing showed a significant saving over single glazing in annual auxiliary energy consumed (~24%) in maintaining similar comfort levels ($PPD_{10}^{+} + PPD_{10}^{-}|_{single}$~ 8%,$PPD_{10}^{+} + PPD_{10}^{-}|_{double}$~ 7% ). However, triple glazing showed no improvement over double glazing in annual auxiliary energy demand, requiring less heating but more lighting. An explanation for this might be that the extra transmittance of the double glazing (~15%), which allows more sun into the room, makes up for its lower insulation value on this climate file. A simple U-value calculation suggests that ~48 Btu/ft$^2$·h (150 W) insolation is required per time period for the extra solar gains associated with double glazing to overcome its lower insulation contribution. Of course, insolation is only available at certain times of the day and account has to be taken of heat stored in the building mass to assess the effect for a whole day but sunlight well in excess of 48 Btu/ft$^2$·h (150 W) is certainly prevalent on many days, suggesting that the above explanation is valid. Figure 8 shows that at higher glazing ratios triple glazing does prove energetically beneficial, consuming about 8% less auxiliary energy than double glazing.

### Glazing Area

Next, an attempt was made to discover the best glazing area for the south facade. Due to the limitations of the nodal network glazing could only be altered in increments of one-ninth of the south facade area and this was done so that symmetry of the glazing about the central vertical axis of the south facade was maintained; double glazing was employed throughout this series of runs; the results are illustrated in Figure 5.

It is apparent that the best glazing area from the point of view of energy consumption is ~30%. This minimum is not particularly well pronounced, the difference between best and worst being ~ 6%, but there are other advantages to using lower glazing areas, as shown in Figure 6.

Overheating is seen to be a problem for higher glazing fractions, with $PPD_{10}^{+}$ exceeded for over 20% of the chosen year. While it is true that much of this overheating will take place during periods of no or infrequent occupancy (results weighting 0.33) and that the worst periods of overheating ($PPD_{10}^{+} > 50\%$ with high glazing fractions during some summer days) are no more extreme than the worst periods of underheating, overheating is much harder to cure; if air conditioning is available at all it is energy intensive and is therefore more disturbing to occupants.

A few runs were performed using triple glazing, which showed the minimum in energy consumption to occur at higher glazing fractions, as might be expected. The general standard of comfort in the triple-glazed room of glazing fraction 0.56 was slightly better than that in the double-glazed case, almost all of this benefit appearing in a reduction in $PPD_{10}^{-}$ (double 13%, triple 11%).

### The Thermostat

Two runs were performed in which air temperature and human index temperature, respectively, were used as the thermostat's response temperature. By setting the thermostat to the same constant value in both cases 70 °F (21 °C) (remember, in all the above runs the thermostat was allowed to vary with preferred temperature) it is possible to get some idea of the impact of using comfort as a way of controlling the thermostat.

Figure 7 clearly illustrates that thermostating to human index temperature is ~29% more costly in energy terms. Since the human index temperature is 46% MRT, which is generally lower than the mean air temperature, this was to be expected. Again expected is the fact that the human index temperature thermostat reduces $PPD_{10}^{+} + PPD_{10}^{-}$.

Glazing Distribution

One of the great advantages of this model is that it allows the user to change variables spatially as well as in magnitude. Using double glazing and keeping the south facade glazing fraction constant (0.33), we now examine the influence of the positioning of this glazing on the south facade. The results are presented in Figure 8.

The savings to be gained by optimizing the glazing distribution are small (~2% annual auxiliary energy consumption separates the best and worst cases) and appear to be influenced by the positioning of the thermal mass in the room. The best performer is distribution 23d. The window positioning in 23d directs incident sunlight onto the floor, which is of relatively high thermal mass; though the reduced heating requirement is compensated by the increase in artificial lighting demanded. The worst performer is 23b, where the windows direct morning sun onto the west wall, an internal wall of low thermal mass.

## CONCLUSIONS

Initial runs with the thermal model *FENESTRA* indicate that for a south-facing room in the UK climate triple glazing offers few advantages over double glazing in terms of auxiliary energy consumed and comfort levels attained except at very high glazing fractions. If double glazing is to be used the suggested optimum glazing fraction is around 30%, and around 50% for triple glazing, though both these minima are shallow.

For a fixed glazing fraction *FENESTRA* suggests that the distribution of glazing on the south facade has a bearing on the auxiliary energy consumed by the room. General advice would be to arrange the windows so that sunlight falls on the higher-mass elements for most of the time.

Implicit in the above analysis of performance based on energy consumption is the comfort of the occupants since the thermostat for occupancy periods was set to respond to a human index temperature and to keep such a temperature at the value at which most people would be most comfortable. It is found that if we revert to a traditional thermostat, responding to air temperature and attempting to keep that air temperature at a constant value around the mean of the preferred temperature, the savings in energy can be substantial but that the comfort of the room's occupants is compromised.

In the future a term for sunlight directly incident on room occupants will be included in the comfort calculation, enabling more detailed comfort mapping on a day to day basis to be performed.

## REFERENCES


Alamdari, F., and Hammond, G.P. 1983. "Improved data correlations for buoyancy driven convection in rooms." BSERT, Vol. 4, No. 3, pp. 106-112.

Alder, K., et al. 1984. "Energy balance and thermal comfort in passive solar housing." First EC Conference on Solar Heating, Amsterdam, pp. 386-390.

ASHRAE. 1977. ASHRAE handbook--1977 fundamentals, chapter 26. New York: American Society of Heating, Refrigerating, and Air-Conditioning Engineers, Inc.

Carroll, J.A. 1980. "An index to quantify thermal comfort in homes." Fifth National Passive Solar Conference , Amherst, pp. 1210-1214.

Clarke, J.A. 1985. Energy simulation in building design. Bristol: Hilger.

CEC. 1986. European passive solar handbook. Brussels: Commission of the European Communities

Geiger, R. 1965. The climate near the ground. Cambridge: HUP.

Heerwagen, D.R., et al. 1979. "The use of a computer routine to assess human thermal comfort for passive-hybrid building designs." Third National Passive Solar Conference San Jose, pp. 134-145.

Hopkinson, R.G., et al. 1966. Daylighting. London: Heinemann.

Howarth, A.T. 1985. "The prediction of air temperature variations in naturally ventilated rooms with convective heating." BSERT, Vol. 6, No. 4, pp. 169-175.

Humphreys, M.A. 1974. "Environmental temperature and thermal comfort." BRE CP 80/74. Garston: Building Research Establishment.
Humphreys, M.A. 1978. "Outdoor temperatures and comfort indoors." BRE CP 53/78. Garston: Building Research Establishment.
Judkoff, R.D. 1988. "Validation of building energy analysis simulation programs at SERI." Energy and Buildings, Vol. 10, pp. 221-240.
Liebecq, G., and Marret, D. 1984. Institute of heating, ventilation and air protection seminar. University of Silesia, Poland.
Littler, J.G.F. 1982. "Overview of some available models for passive solar design." Computer Aided Design, Vol. 14, No. 1, pp. 15-18.
Martin, C. 1988. Private Communication with authors.
Martin, C., and Watson, M. 1988. "Measurement of convective heat transfer coefficients in realistic room geometry." EMC. Cranfield: Energy Monitoring Co.
McIntyre, D.A. 1980. Indoor climate, pp. 240-. London: Applied Science Publishers.
Nevrala, D.J., and Pimbert, S.L. 1981. "Living Room and bedroom temperatures in homes." BSERT, Vol. 2, No. 3, pp. 109-118.
Ruberg, K. 1979. "Heat distribution by natural convection: modelling procedure for enclosed spaces." Third National Passive Solar Conference ,San Jose, pp. 224-230.
Welty, J.R. 1978. Engineering heat transfer, chapter 6. New York: Wiley.

TABLE 1

Construction Details of the Modeled Room

| Boundary | Construction |
|---|---|
| south wall | 3.9 in (100 mm) brick + 3.9 in (100 mm) insulation + 3.9 in (100 mm) blockwork + 0.5 in (13 mm) plaster |
| north wall | 0.5 in (13 mm) plaster + 3.9 in (100 mm) light concrete |
| east/west walls | 0.5 in (13 mm) plaster + 3.0 in (75 mm) plasterboard |
| ceiling | 0.5 in (13 mm) plasterboard + 5.9 in (150 mm) light concrete |
| floor | 0.9 in (20 mm) carpet + 2 in (50 mm) screed + 3.9 in (100 mm) concrete + 2 in (50 mm) sand + 5.9 in (150 mm) hardcore |

TABLE 2

The Validity of the Chosen 36-Day Weather Data Set

| | ave. max. daily temp.(°F) | ave. min. daily temp.(°F) | ave. max. sth. global insol.(Btu/ft$^2$.hr) | ave. max. daily wind speed(ft/s) |
|---|---|---|---|---|
| 365 days | 57.2 | 45.7 | 102 | 20.0 |
| 36-day sample | 57.2 | 45.5 | 99 | 20.7 |

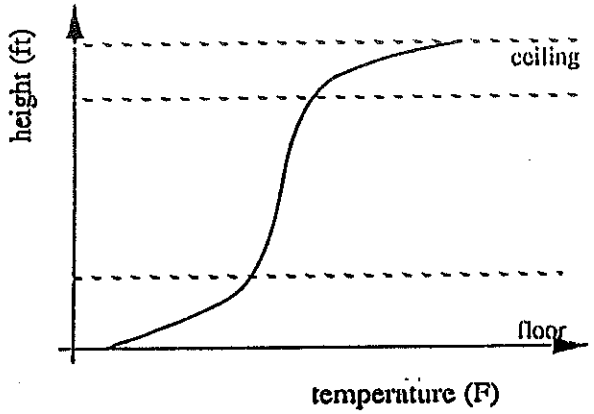


*Figure 1. Typical observed stratification profile for a domestic room*

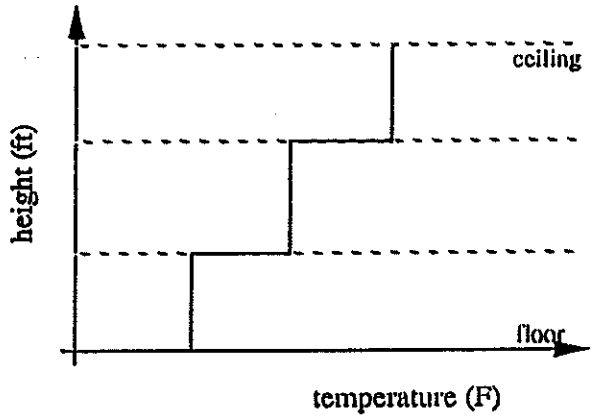


*Figure 2. A typical stratification profile calculated by FENESTRA (compare with Fig. 1)*

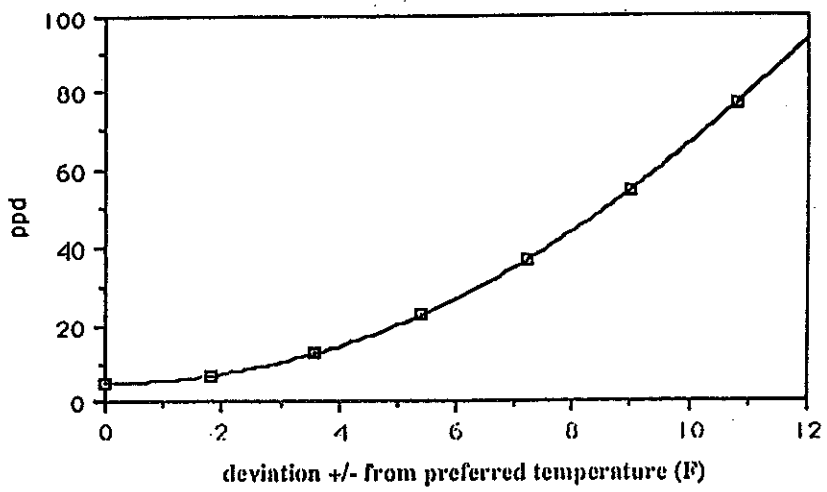


*Figure 3. The approximate quadratic form of Fanger's PPD curve*

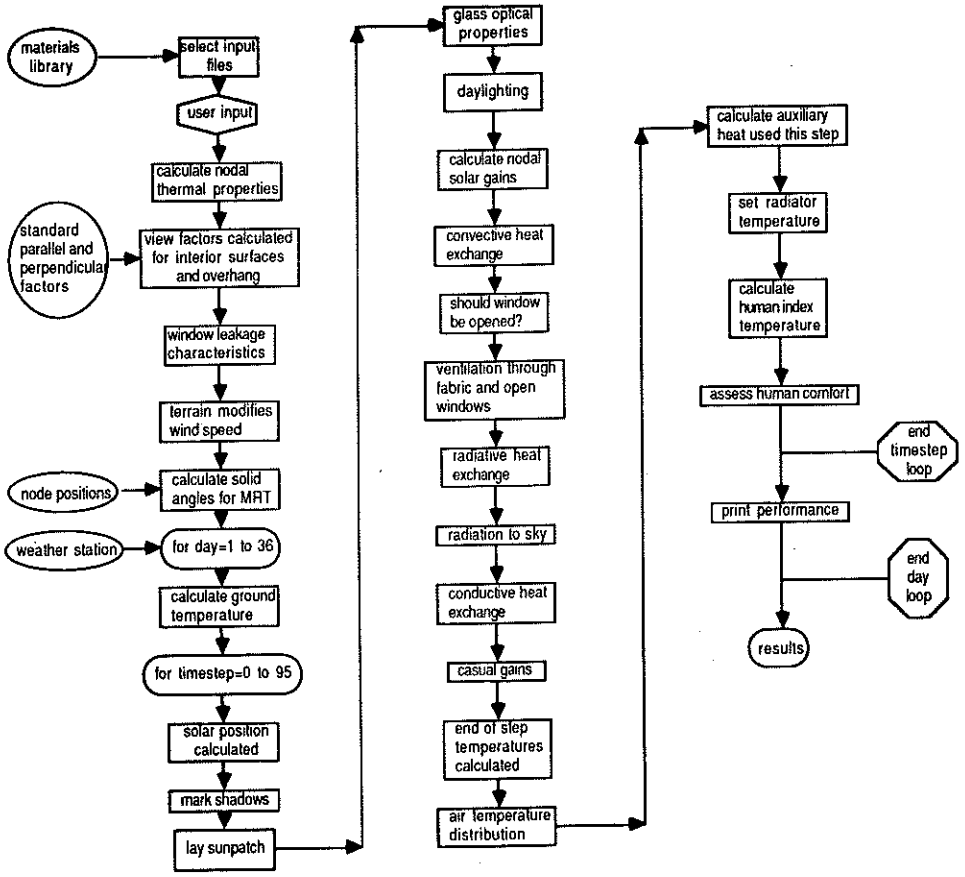


***Figure 4.*** *A flow diagram for FENESTRA's "engine"*

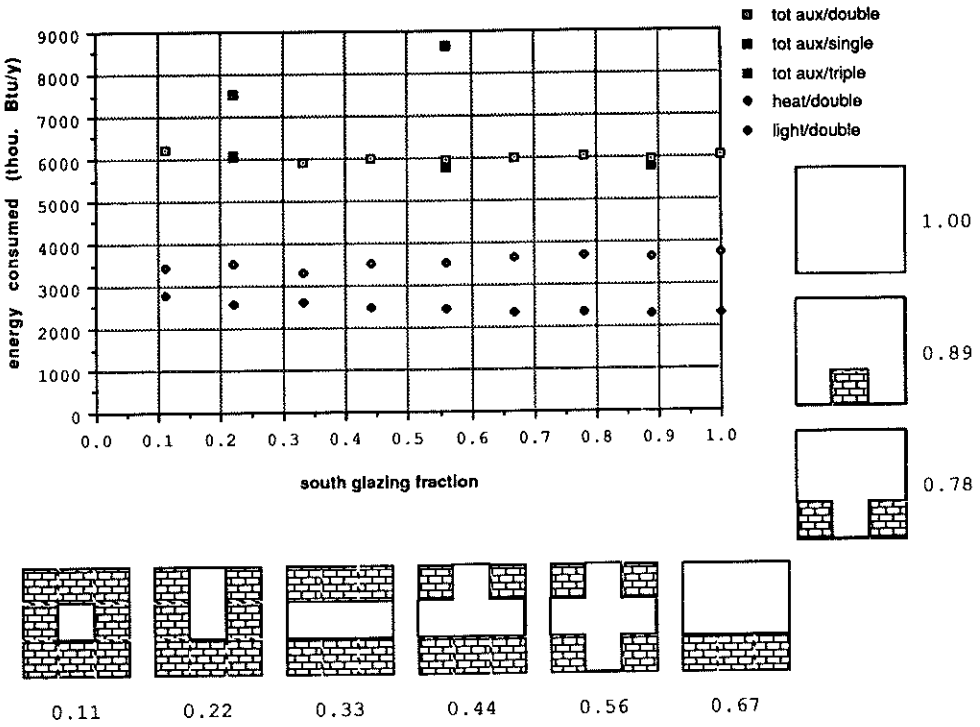


***Figure 5.*** *Annual auxiliary energy demand as a function of the south facade glazing fraction*

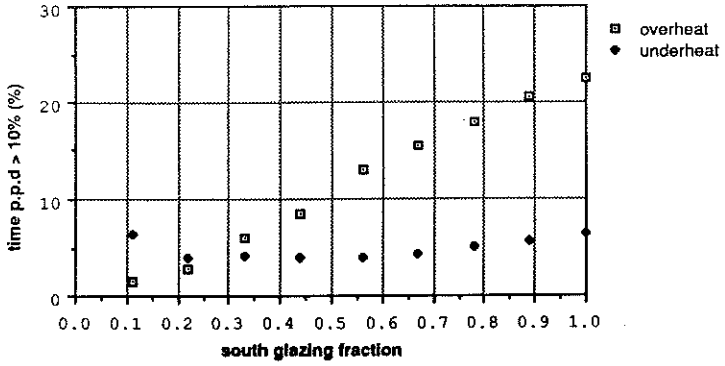


***Figure 6.*** *% of time that PPD is greater than 10% due to overheating or underheating as a function of the south facade glazing fraction with the number of glazed layers held constant (double)* .

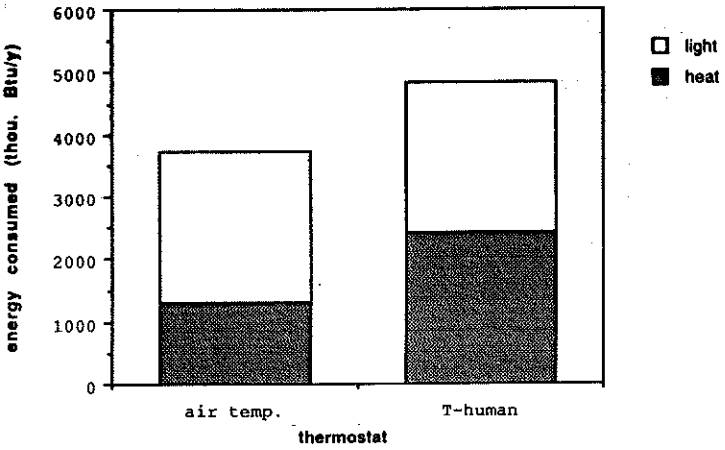


***Figure 7.*** *Annual auxiliary energy demand as a function of thermostat response temperature with the number of glazed layers and south facade glazing fraction held constant (double, 0.55)*

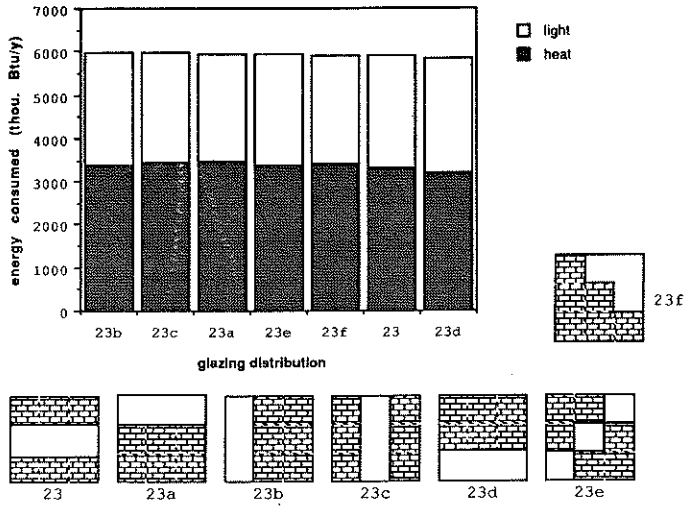


***Figure 8.*** *Annual auxiliary energy demand as a function of glazing distribution with the number of glazing layers and south facade glazing fraction held constant (double, 0.33)*